European Journal of Pharmacology 602 (2009) 124–131

Contents lists available at ScienceDirect

European Journal of Pharmacology

journal homepage: www.elsevier.com/locate/ejphar

Cardiovascular Pharmacology

# Zoledronate inhibits the proliferation, adhesion and migration of vascular smooth muscle cells

Liang Wu [a], Lei Zhu [a], Wei-Hao Shi [a], Jin Zhang [b], Duan Ma [b], Bo Yu [a,*]

[a] General Surgery of Huashan Hospital, Shanghai Medical College, Fudan University, Shanghai 200040, China
[b] Key Laboratory of Molecular Medicine, Ministry of Education, Shanghai Medical College, Fudan University, Shanghai 200032, China

ARTICLE INFO

*Article history:*
Received 30 April 2008
Received in revised form 23 September 2008
Accepted 15 October 2008
Available online 31 October 2008

*Keywords:*
Zoledronate
Bisphosphonates
Vascular smooth muscle cells
Intimal hyperplasia
Atherosclerosis

ABSTRACT

Bisphosphonates, which are extensively used in bone-related disorders, have been reported to inhibit atherosclerosis and neointimal hyperplasia. In the present study, we investigated the effects of a bisphosphonate, zoledronate, on the proliferation, adhesion, migration and microstructure of vascular smooth muscle cells (VSMCs) from Sprague–Dawley rats. It was shown that zoledronate suppressed VSMCs proliferation after 48 h cultivation in a dose depend manner, most obviously at concentrations above 10 μM. Cell cycle analysis indicated that zoledronate inhibited the proliferation of VSMCs via cell cycle arrest at S/G2/M phase. This inhibition was not associated with cell death. In a modified Boyden chamber model, it was shown that zoledronate dose-dependently inhibited VSMCs adhesion to collagen and migration stimulated by platelet-derived growth factor-BB. Western blot analysis suggested that zoledronate significantly inhibited the phosphorylation of focal adhesion kinase. Furthermore, we observed that more and more VSMCs changed from a bipolar appearance to a globular shape under inverted light microscope as zoledronate concentration increased from 0.1 to 100 μM. Images under transmission electron microscope confirmed this morphological change, and many electron density bodies were observed in zoledronate-treated VSMCs. These findings indicated that bisphosphonates' effects of suppressing atherosclerosis and neointimal hyperplasia might be due to inhibition of VSMCs, at least for zoledronate.



## 1. Introduction

Bisphosphonates have been used widely in the treatment of disorders associated with excessive bone resorption, such as hypercalcemia of malignancy, multiple myeloma, osteoporosis and Parget's disease (Lortholary, 2001; Peest and Ganser, 2007; Owens et al., 2007; Merlotti et al., 2007). They are stable analogues of inorganic pyrophosphate, an endogenous regulator of calcium metabolism that prevents ectopic calcification (Tenenbaum et al., 1992). The half-life of bisphosphonates in the circulation is short, and they enter rapidly and extensively into bone because of their high affinity to the calcium and hydroxyapatite crystals, then inactivate osteoclasts which are monocyte–macrophage origin that regulate bone resorption.

Bisphosphonates have also been reported to accumulate markedly in the aortas of both healthy and atherosclerotic rabbits in vivo (Ylitalo et al., 1996) and in human internal mammary arteries in vitro (Ylitalo et al., 1998). Increasing studies have shown that bisphosphonates could inhibit the development of experimental atherosclerosis (Daoud et al., 1987; Ylitalo et al., 1994) and neointimal hyperplasia (Hoch et al., 1999; Danenberg et al., 2002). These effects were mostly attributed to the transient systemic inactivation of monocytes and macrophages which have strong phagocytic capabilities. Effects of bisphosphonates on non-phagocyting vascular smooth muscle cells (VSMCs), of which proliferation, adhesion and migration play rather important roles in atherosclerosis and neointimal hyperplasia, were no or minor, even if bisphosphonates were encapsulated in liposomes or nanoparticles to facilitate membrane penetration (Danenberg et al., 2003; Cohen-Sela et al., 2006; Epstein et al., 2007). Thus, researchers contributed the reduction of VSMCs layers to reduced local inflammation and subsequent inhibition of VSMCs growth.

Zoledronate is a member of the newest generation of bisphosphonates and suggested to have the most potent antiresorptive effects tested (Green, 2002). In this study we characterized its effects on Sprague–Dawley (SD) rat aortic VSMCs proliferation, adhesion and migration. Furthermore, the microstructure changes of VSMCs treated with zoledronate were analyzed by using light microscope and transmission electron microscope. It is concluded that zoledronate inhibits the proliferation, adhesion and migration of VSMCs, and these results may contribute to a better understanding of the mechanisms of bisphosphonates suppressing atherosclerosis and neointimal hyperplasia.

* Corresponding author. Box 37w, 12 Mid Urumqi Rd, Shanghai 200040, China. Tel.: +86 21 62489999 6905; fax: +86 21 62489191.
*E-mail addresses:* yubo120@hotmail.com, 062105353@fudan.edu.cn (B. Yu).

0014-2999/$ – see front matter © 2008 Elsevier B.V. All rights reserved.
doi:10.1016/j.ejphar.2008.10.043

## 2. Materials and methods

### 2.1. Materials

Zoledronate was kindly provided by Novartis Pharma AG (Stein, Switzerland). RPMI 1640 medium with 2 mmol/L L-glutamine was purchased from Biowest (Nuaille, France). Fetal bovine serum (FBS) was purchased from PAA Laboratories GmbH (Linz, Austria). Murine recombinant platelet-derived growth factor-BB (PDGF-BB) was purchased from PeproTech Inc. (Rocky Hill, USA). Crystal violet was purchased from Sigma (St. Louis, USA). Tissue culture disposable material was purchased from NUNC (Roskilde, Denmark). Transwell with 8-μm pore polycarbonate membrane was purchased from Corning (NY,USA). Monoclonal antibody to alpha-smooth muscle actin was purchased from Dako Cytomation (Glostrup, Denmark). Fluorescein conjugated Affinipure goat anti-mouse IgG was purchased from Protein Tech Group Inc (Chicago, USA). Polyclonal rabbit anti-focal adhesion kinase (FAK) Tyr-861 antibody and phosphospecific polyclonal antibody to FAK Tyr-861 were purchased from Signalway Antibody (Pearland, USA). All other chemicals and reagents were obtained from commercial sources and were of analytical grade.

### 2.2. Cell culture

VSMCs were isolated from the thoracic aorta of SD rats by using the method described previously (Hou et al., 2004). Cells were grown in RPMI 1640 supplemented with 10% heat-inactivated FBS, 100 U/ml penicillin and 100 μg/ml streptomycin. Cultures were maintained at 37 °C in a humidified 95% air and 5% $CO_2$ atmosphere. A hill and valley pattern, typical of cultured VSMCs, was seen when the cells reached confluence. VSMCs type and purity were further confirmed in culture by immunohistochemistry with monoclonal antibody to alpha-smooth muscle actin and fluorescein conjugated secondary antibody, which showed more than 95% positive staining of the cells (data not shown). VSMCs were passaged by trypsinization with 0.02% EDTA and 0.25% trypsin in $Ca^{2+}$ and $Mg^{2+}$ free Dulbecco phosphate-buffered saline (PBS). In this study, early passaged (four to eight) VSMCs were used for the experiments and made quiescent by serum starvation in 0.4% FBS for 24 h.

### 2.3. Cell proliferation and morphometric analysis by light microscopy

VSMCs ($2\times10^4$ cells/plate) were seeded in 24-well plates, after quiescent VSMCs were inoculated into RPMI 1640 containing 10% FBS with or without increasing concentrations (0.1–100 μM) of zoledronate for 48 h and visually inspected by Olympus CKX41 inverted phase contrast microscope (Tokyo, Japan). Cells in RPMI 1640 plus 10% FBS alone served as a control. After treatment, cells were obtained by trypsinization, and cell numbers were counted using a Beckman Coulter Z2 Series counter (Florida, USA), assessing three counts for each well and a mean value taken. Triplicate wells were assessed for each treatment, experiments were done three times. Results were compared with control cells.

### 2.4. Ultrastructure analysis by transmission electron microscopy

After treated with or without zoledronate (100 μM) for 48 h, cells were harvested with a scraper and sedimented by centrifugation at 2500 rpm for 5 min at 4 °C. The pellet was suspended in PBS containing 2.5% gluteraldehyde for 1 h, fixed cells were rinsed three times in PBS and post-fixed with 1% $OsO_4$ for 1 h. Then the cells were dehydrated in a series of ethanol, and embedded in Epon. Ultrathin sections were cut, double stained with uranyl acetate and lead citrate, and examined under a Philips CM 120 transmission electron microscope (Eindhoven, Netherlands) at 60 kV.

### 2.5. Cell cycle distribution assays

To analyze the cell cycle distribution of VSMCs exposed to zoledronate, cells were seeded in 25 $cm^2$ tissue culture flasks and treated with or without zoledronate (100 μM) for 48 h. After treatment, the adhered cells were obtained by trypsinization and pooled with the floating cells and centrifuged at 2000 rpm for 5 min. The cells were washed with PBS before fixation in citric acid. After the fixation, cells were treated with 0.1 mg/ml DNase-free RNase in 1 ml of PBS for 30 min at 37 °C, resuspended in 0.05 mg/ml propidium iodide and then analyzed for DNA content with the use of flow cytometry (FACScan cytometer, CellQuest software, Becton Dickinson).

### 2.6. Hoechst 33258 staining

Cells were seeded in a 24-well plate and treated as described for the proliferation studies. After treatment, cells were fixed, washed twice with PBS and stained with Hoechst 33258 staining solution for 5 min at room temperature and observed under fluorescence microscope using a 4′, 6-diamidino-2-phenylindole (DAPI) filter. Fragmented or condensed nuclei were scored as apoptotic.

### 2.7. Double staining of annexin V and propodium iodide

Cells were stained with annexin V and propodium iodide and then evaluated for apoptosis by flow cytometry according to the manufacturer's protocol (BD Biosciences). Briefly, cells were collected, washed twice with cold PBS, and centrifuged at 2000 rpm for 5 min. Cells were resuspended in 0.4 ml binding buffer at a concentration of $1\times10^6$ cells per ml, 0.1 ml of the solution was transferred to a 5 ml culture tube, and 5 μl of annexin V and 5 μl of propodium iodide were added. Cells were gently vortexed and incubated for 15 min at room temperature in the dark. Finally, 400 μl of binding buffer was added to each tube, and samples were analyzed by FACScan flow cytometer. For each sample, 10,000 ungated events were acquired.

Cells in the lower right quadrant correspond to early apoptotic cells (annexin V-positive and propodium iodide-negative), whereas those in the upper right quadrant correspond to late apoptotic or necrotic cells (annexin V- and propodium iodide-positive).

### 2.8. Cell adhesion

The effect of zoledronate on VSMCs adhesion was assayed with Transwell, 24-well tissue culture plates comprising an intervening 8-μm pore polycarbonate membrane separating the upper and lower wells. The upper side of the membrane was coated with 20 μg/mL collagen type I to promote cell adhesion. Cells were divided into

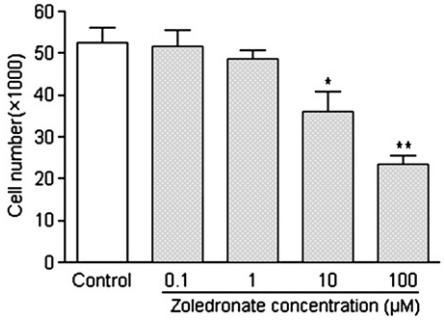


**Fig. 1.** Effect of zoledronate on VSMCs proliferation. Cells ($2\times10^4$) were seeded per well and counted in a Coulter counter after 48 h of culture in the presence or absence of indicated concentrations of zoledronate. Results are means ± S.D. of three independent experiments. * and ** indicate $P<0.05$ and $P<0.01$ respectively, compared with the control.

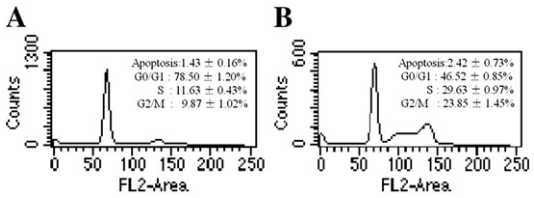


**Fig. 2.** Flow cytometric analysis of DNA content for zoledronate-treated VSMCs. Cells were incubated for 48 h, either in the absence (A) or in the presence of zoledronate at a concentration of 100 μM (B). Cells were harvested, fixed and stained with propidium iodide. Results are means ± S.D. of three independent experiments.

aliquots of $1\times10^4$ cells resuspended in serum free medium with or without increasing concentrations (0.1–100 μM) of zoledronate. Cells in serum free medium alone served as a control. Chambers were incubated for 1 h at 37 °C. Next, the membrane's upper portion was rinsed, fixed, and stained with crystal violet dye. Adhesion was assessed by counting the number of cells per three independent high-power fields (HPFs ×400) with light microscope.

### 2.9. Cell migration

The effect of zoledronate on VSMCs migration was also monitored with Transwell using a modified Boyden's chamber assay. Briefly, the cells were harvested by trypsinization and suspended in the serum free RPMI 1640 supplemented with 0.2% BSA. Cell suspensions were then placed into the upper well at a concentration of $1\times10^4$ cells/100 μl, while the same medium was placed into lower well (600 ml). PDGF-BB (10 ng/ml) and zoledronate at various concentrations were added only to the lower compartment of the chamber. Serum free medium containing 0.2% BSA and 10 ng/ml PDGF-BB served as a control. The chamber was incubated at 37 °C in 5% $CO_2$ humidified atmosphere for 4 h. Non-migrating cells on the upper surface were scraped gently and washed out with PBS for 3 times. VSMCs migrated to the lower surface of the membrane were stained with crystal violet dye and counted per three independent HPFs (×400) with light microscope.

### 2.10. Western-immunoblot analysis

After VSMCs were treated with or without increasing concentrations (0.1–100 μM) of zoledronate for 24 h, cell layers were rinsed three times with PBS and extracted in ice-cold lysis buffer (150 mM NaCl, 50 mM Tris–HCl, pH 7.4, 1 mM EDTA, 1 mM Na3VO4, 1 mM NaF, 1% NP-40, 0.1% SDS, 1 mM PMSF, 1 mg/ml each of aprotinin, leupeptin, pepstatin) for 10 min. Lysates were centrifuged at 12,000 rpm for 5 min at 4 °C, and supernatants were stored at −80 °C. Protein concentrations were determined by the BCA method. Twenty micrograms of protein from each cell extract was separated by electrophoresis on 10% SDS-polyacrylamide gels and then transferred to Polyvinyl difluoride (PVDF) membrane (Amersham Biosciences Europe, Freiburg, Germany). Membranes were blocked with blocking solution (50 mM Tris–HCl, 150 mM NaCl, 5%(w/v) non-fat dry milk and 0.1%Tween 20) overnight at 4 °C, and immunoblotted with rabbit antibody to FAK Tyr-861 (1:1000), and p-FAK Tyr-861 (1:1000). Horseradish peroxidase-conjugated goat anti-rabbit IgG was used at 1:10,000 dilution for 1 h. The proteins were visualized using Immobilon Western detection reagents (Millipore).

### 2.11. Statistical analysis

Data were expressed as mean ± S.D. of three independent experiments. Statistical differences were evaluated using the Student's *t*-test and considered significant at $P<0.05$ or $P<0.01$ level. Figures shown in this article were obtained from at least three independent experiments with similar results.

## 3. Results

### 3.1. Effect of zoledronate on VSMCs proliferation

The effects of various concentrations of zoledronate on the proliferation of VSMCs were studied by measuring the cell number in the absence or presence of zoledronate at different concentrations after 48 h incubation. As described in Fig. 1, zoledronate had minor effects on VSMCs proliferation at low concentrations (<1 μM). In contrast, cell numbers were significantly reduced at concentration above 10 μM ($P<0.01$). The inhibitive rate was 89.6% when VSMCs were treated with 100 μM zoledronate.

### 3.2. Effect of zoledronate on VSMCs cell cycle distribution assays

To further examine whether the decrease in proliferation of VSMCs reflected a cell cycle arrest, cell cycle progression was analyzed by propidium iodide staining and FACS analysis. The controlled VSMCs revealed a cell-cycle distribution typical of that fast proliferating cells, with an average of 78.5% of cells exhibiting a 2n DNA content (G0/G1 phase), 11.6% of cells featuring a 4n DNA content (G2/M phase) and 9.9% revealing a DNA content of between 2n and 4n (S phase).

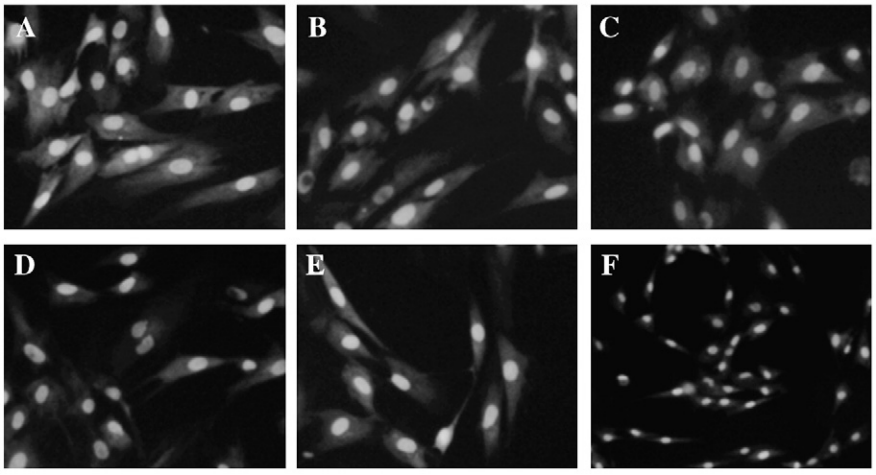


**Fig. 3.** Nuclear staining of VSMCs by Hoechst 33258. VSMCs were treated without (A) or with 0.1 (B), 1 (C), 10 (D), 100 μM (E and F) of zoledronate for 48 h. A–E (magnification, ×400), F (magnification, ×100). The results shown are representative of three separate experiments.

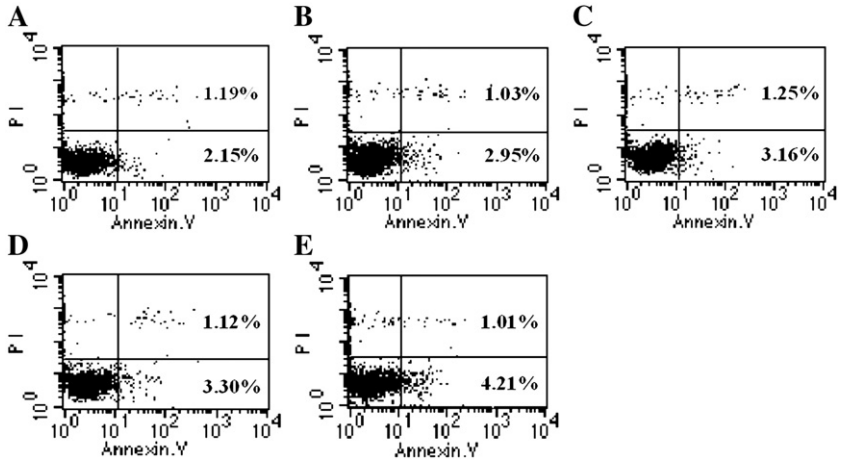


**Fig. 4.** Double staining of annexin V and propodium iodide. Cells were treated without (A) or with 0.1 (B), 1 (C), 10 (D), 100 μM (E) of zoledronate for 48 h. The presence of apoptic cells was identified by flow cytometric analysis of cells labeled with annexin V and propidium iodide. Cells in the lower right quadrant correspond to early apoptotic cells, whereas those in the upper right quadrant correspond to late apoptotic or necrotic cells. Numbers in each quadrant are percentage of cells they contain. The results shown are representative of three separate experiments.

After treatment of VSMCs with 100 μM zoledronate for 48 h, the G0/G1 phase occupied only 46.5% of the cell cycle, by contrast, cells in G2/M and S phase increased to 29.6% and 23.9%, respectively. Additionally, no obvious apoptotic cells were detected in zoledronate treated VSMCs (Fig. 2). The results indicated that zoledronate down-modulated VSMCs proliferation via cell cycle arrest at the S/G2/M phase.

### 3.3. Effect of zoledronate on VSMCs apoptosis

In order to verify if the induction of apoptosis occurred during zoledronate treatment, the presence of apoptotic cells was determined by means of Hoechst 33258 staining, and the application of double staining with annexin V and propodium iodide. Hoechst 33258 staining assay showed that fragmented or condensed nuclei were rarely seen in VSMCs following zoledronate treatment. Also, flow cytometry assays revealed that treatment of VSMCs with various concentrations of zoledronate for 48 h caused only minimal apoptosis versus control. Taken together, these results indicated that zoledronate was not affecting VSMCs proliferation through increasing cell apoptosis. Representative results of Hoechst 33258 assays are shown in Fig. 3 and flow cytometry assays are shown in Fig. 4.

### 3.4. Effect of zoledronate on VSMCs microstructure

As the concentration of zoledronate increased from 0.1 to 100 μM, increasingly more VSMCs retracted from the substratum and lost contacts between neighboring cells, but still attached to the culture plate (Fig. 5), which appeared to be more globular in shape. Although these morphological changes were noted, no deleterious effects on cellular viability were observed.

To further explore the ultrastructure changes of VSMCs treated with zoledronate, the ultrathin sections of VSMCs treated with or without zoledronate (100 μM) were examined under a transmission electron microscope. Untreated cells exhibited the typical spindle shape (Fig. 6A) with a diverse array of intracellular organelles that included well-developed rough endoplasmic reticulum, Golgi apparatus, mitochondria, and nuclei (Fig. 6D). VSMCs treated with

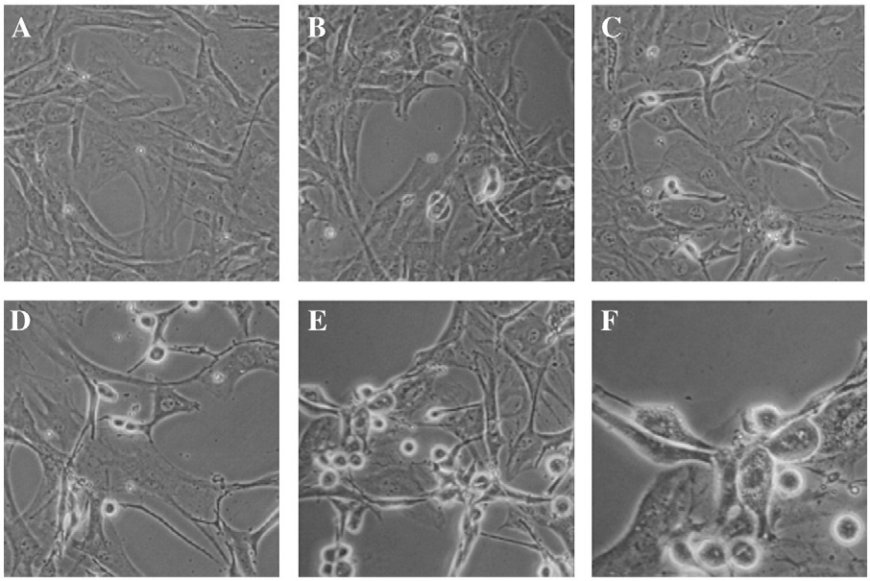


**Fig. 5.** Zoledronate effects on VSMCs morphology after 48 h using light microscope. VSMCs were treated without (A) or with 0.1 (B), 1 (C), 10 (D), 100 μM (E and F) of zoledronate for 48 h. Cells were viewed under Olympus CKX41 inverted phase contrast microscope. Note the change in shape of VSMCs from bipolar to globular when exposed to zoledronate. A–E (magnification, ×200), F (magnification, ×400).

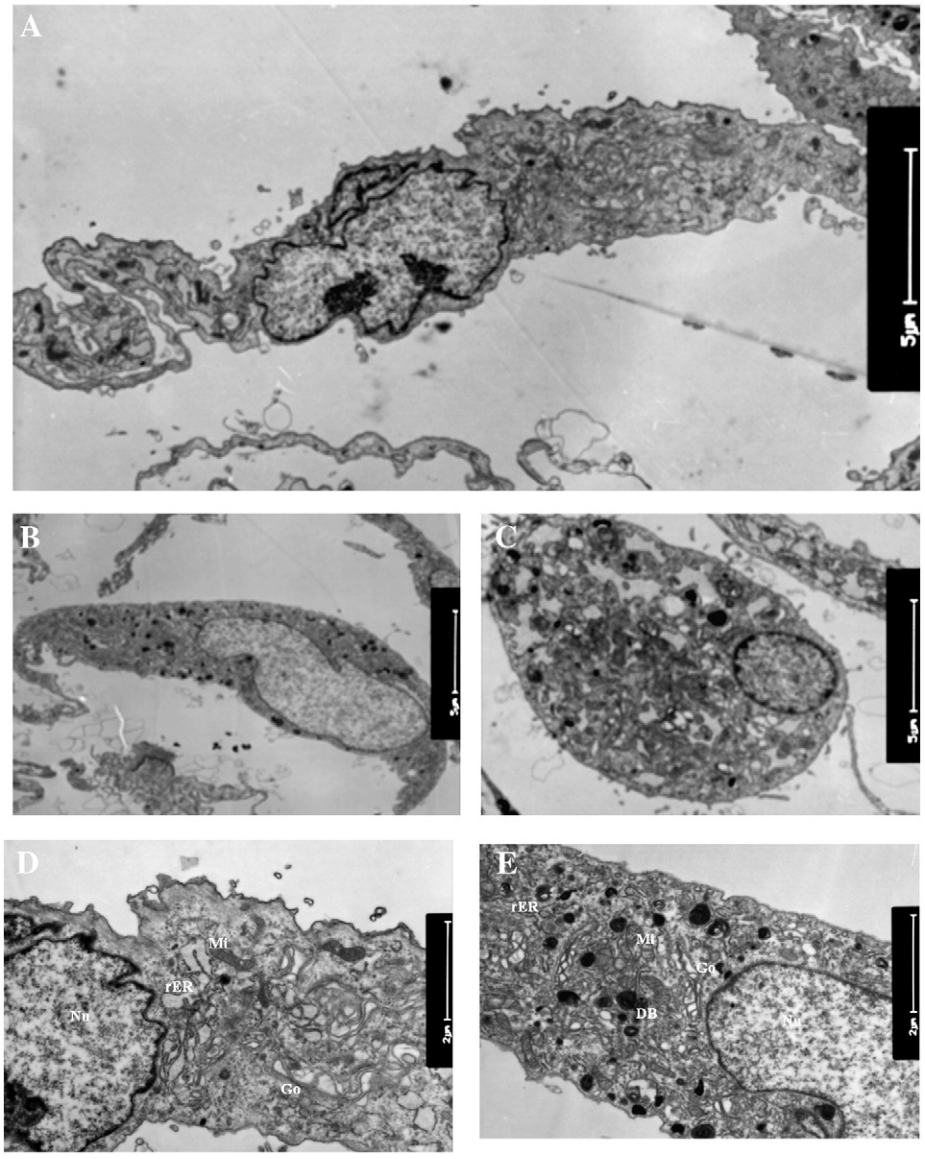


**Fig. 6.** Electron microscopy images showing ultrastructural features of a control cell (A, D) and coexistence of morphological features of cells (B, C, E) exposed to zoledronate (100 μM). D and E are higher power images of A and B respectively. A, Low-power image of untreated cells exhibited the normal appearance of spindle shape; B and C, Low-power images of VSMCs treated with zoledronate for 48 h exhibited the characteristic ultrastructural morphology of a more globular shape; D, High-power image of untreated cells shows a diverse array of intracellular organelles that include well-developed rough endoplasmic reticulum (rER), Golgi apparatus (Go), mitochondria (Mi), and nuclei (Nu); E, High-power image of VSMCs treated with zoledronate shows large amounts of electron density bodies (DB).

zoledronate showed the more globular shape (Fig. 6B–C). In addition, large amounts of high electron density bodies (lysosomes) were observed in the cytoplasm (Fig. 6E).

### 3.5. Effect of zoledronate on VSMCs adhesion to collagen

Adherence of cells to the underlying matrix is believed to be an essential component in cell movement and the development of hyperplastic vascular lesions. To determine the effects of zoledronate on VSMCs adhesion to collagen type I, cell counts were determined after incubated for 1 h. As shown in Fig. 7, zoledronate inhibited VSMCs adhesion in a concentration-dependent manner. In the presence of 100 μM zoledronate, the mean number of adhered cells was only 31.6% of the control cells.

### 3.6. Effect of zoledronate on VSMCs migration

PDGF-BB released from restenotic or atherosclerotic lesions acts as a chemoattractant and proliferative agent for VSMCs (Delafontaine,

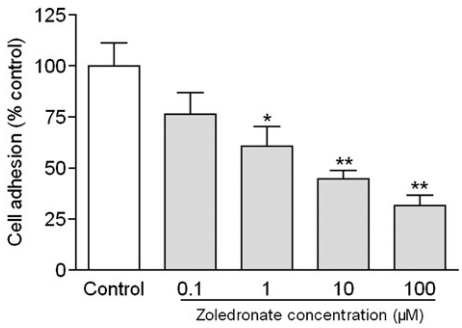


**Fig. 7.** Effect of zoledronate on VSMCs adhesion. Cells ($1 \times 10^4$) were seeded per well and counted after 1 h of culture in the presence or absence of indicated concentrations of zoledronate. Results are means ± S.D. of three independent experiments. * and ** indicate $P<0.05$ and $P<0.01$ respectively, compared with the control.

1998). To determine the effect of zoledronate on PDGF-BB-stimulated VSMCs migration, we carried out migration assays in the presence of 10 ng/ml PDGF-BB and zoledronate at various concentrations. As shown in Fig. 8, PDGF-BB induced VSMCs migration more than 4-fold as compared with unstimulated control cells. 0.1 μM zoledronate had little effect on PDGF-BB-stimulated migration. However, above 1 μM zoledronate inhibited PDGF-BB-stimulated cell migration efficiently with the increase of zoledronate concentration. In the presence of 100 μM, the number of migrated cells was 40.4% of the PDGF-BB-stimulated control. These results indicated that zoledronate induced a dose-dependent inhibition of PDGF-BB-stimulated VSMC migration.

### 3.7. Effect of zoledronate on phosphorylation of FAK

Phosphorylation of focal adhesion kinase is critical for cell adhesion and migration (Panetti, 2002; Webb et al., 2002). The decline in VSMCs adhesion and migration suggested that zoledronate might be altering the phosphorylation of FAK. To measure FAK phosphorylation, we immunoprecipitated FAK from VSMCs extracts and performed an immunoblot with an antibody to detect phosphorylated tyrosine. As shown in Fig. 9, there was a significant decrease in tyrosine phosphorylation of FAK in comparison with control samples.

## 4. Discussion

It is well established that accelerated proliferation of VSMCs and migration of VSMCs from the media to the intimal are fundamental events in the development of both intimal hyperplasia and atherosclerosis (Hanke et al., 1990; Davies and Hagen, 1994; Ross, 1997; Andres, 1998). In addition, cell-matrix adhesion is known to influence proliferation, migration and survival of VSMCs (Morla and Mogford, 2000; Koutsouki et al., 2005; Kamiya et al., 2007). Therefore, inhibition of VSMCs proliferation, adhesion and migration represents a potentially promising therapeutic strategy for the treatment of diseases such as atherosclerosis and intimal hyperplasia.

Bisphosphonates are the most widely used and effective anti-resorptive agents for the treatment of diseases in which there is an increase in osteoclastic resorption. They are carbon-substituted analogs of pyrophosphate. Based on the absence or presence of a nitrogen atom on the side chains, they can be categorized into two groups. Non-nitrogen-containing bisphosphonates, such as clodronate and etidronate, were the first antiresorptive bisphosphonates to be developed for clinical use. Nitrogen-containing bisphosphonates, such as alendronate and zoledronate, are much more potent at inhibiting bone resorption. The mechanism of bisphosphonate action is now well documented, with nitrogen-containing bisphosphonates like zoledronate inhibiting a key enzyme, farnesyl diphosphate

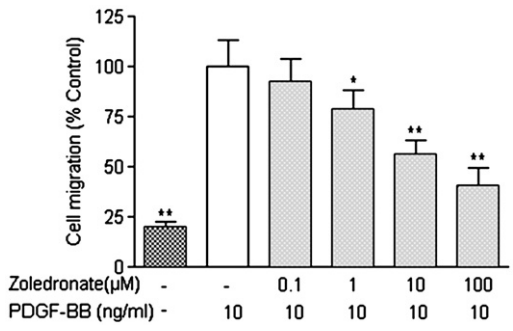


**Fig. 8.** Effect of zoledronate on PDGF-BB-stimulated VSMCs migration. After incubation with zoledronate for 4 h, the numbers of migrated cells were determined along with controls. Results are means ± S.D. of three independent experiments. * and ** indicate $P<0.05$ and $P<0.01$ respectively, compared with the control.

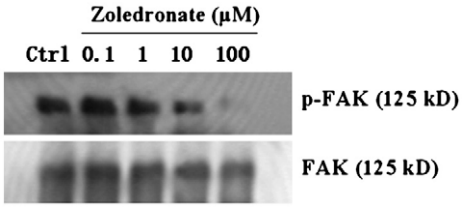


**Fig. 9.** Zoledronate suppressed FAK phosphorylation. VSMCs cultured in the absence or presence of increasing concentrations of zoledronate were lysed in the plates, the amount of tyrosine phosphorylated FAK was reduced in zoledronate treated VSMCs. The results shown are representative of three separate experiments.

synthase (Van Beek et al., 1999), in the mevalonate pathway, this class of bisphosphonates prevents protein prenylation of a wide variety of small intracellular G-proteins, including Ras, Rac, Rab and Rho (Luckman et al., 1998). Loss of prenylation consequently prevents these proteins from acting at the correct spatial location within the cell, thus ultimately affecting their normal behavior, including cell proliferation, survival, cytoskeletal organization and vesicular trafficking (Zhang and Casey, 1996).

Bisphosphonates have also been found to exhibit the effects of inhibiting development of atherosclerosis and neointimal hyperplasia, and etidronate has been reported to inhibit the intima-media thickening of carotid artery even in man (Koshiyama et al., 2000). Bisphosphonates not only bind tightly to hydroxyapatite in the bone but they also concentrate in the arterial wall of both healthy and especially atheromatous rabbits for at least several days or a week (Ylitalo et al., 1996). Thus, this leads to the hypothesis that bisphosphonates might exert direct effects on VSMCs, which are the major cellular components of vascular wall. Thereafter, etidronate was found to inhibit the growth of VSMCs from spontaneous hypertensive rats, but cells from Wistar Kyoto rats were not affected (Su et al., 2002).

In the present study, zoledronate was found to have minor effects on VSMCs proliferation at relative low concentrations after 48 h incubation, but cell numbers were significantly reduced at concentration above 10 μM, and the inhibitive rate reached a maximum 89.6% when VSMCs were treated with 100 μM zoledronate. Similar concentrations (typically 10–100 μM) of zoledronate have been utilized elsewhere to produce anti-proliferative effects against human epidermoid cell lines, leukemia cells and non-small cell lung cancer cells (Caraglia et al., 2004; Ohtsuka et al., 2005; Li et al., 2008). One concern is that the doses required to achieve inhibition of cell growth may not be achieved in vivo using current treatment regimens. A peak serum concentration of zoledronate following a 4 mg dose administration ranges only from 1 to 5 μM (Berenson et al., 2000). It has been suggested however that the effective local concentrations of bisphosphonates at the sites of artery, especially atherosclerotic artery, may be much higher than serum levels. At 24 h after dosing in healthy rabbits, the mean aorta to plasma ratios of clodronate, etidronate, and pamidronate were, respectively, 2.4 to 2.8, 2.4 to 4.0, and 8.6 to 10. The corresponding ratios in atherosclerotic rabbits were, respectively, 13 to 22, 1.5 to 2.2, and 13 to 24 (Ylitalo et al., 1996). It is unclear however if the bioavailability of zoledronate in artery, particularly for VSMCs, would allow effective concentrations above 10 μM. Despite this concern, the low toxicity of bisphosphonates, coupled with promising results from their usage to treat atherosclerosis and neointimal hyperplasia, warrants a more in-depth investigation into the potential effects these drugs may exert directly on VSMCs. More detailed studies on the mechanism of zoledronate mediated inhibition of VSMCs growth using in vivo model systems should further clarify its potential use for improved treatment of atherosclerosis and neointimal hyperplasia.

Previous studies found that zoledronate induced apoptosis in a variety of tumor cell lines, including osteogenic sarcoma cells,

myeloma cells and human pancreatic cancer cells (Evdokiou et al., 2003; Ibrahim et al., 2003; Tassone et al., 2003). To exclude the possibility that zoledronate reduced VSMCs number by causing cell death, we conducted apoptosis assays, which showed only minor increases in the proportions of apoptic cells as zoledronate concentration increased from 0.1 to 100 μM. Cell cycle analysis demonstrated that an accumulation of cells within the S and G2/M phase of the cell cycle after just 48 h of exposure to zoledronate. This result indicated that zoledronate inhibited VSMCs proliferation, at least in part, by arresting cell cycle at the S/G2/M phase. This effect has also been observed in non-small cell lung cancer cells after zoledronate treatment (Li et al., 2008).

Zoledronate also exerted a concentration-dependent effects on the adhesion and migration of VSMCs in vitro, with a reduction about 68.4% and 59.6% respectively in the number of adhered and migrated VSMCs at 100 μM in the indicated time. Other bisphosphonates have been reported to inhibit the binding of a multiple of malignant tumor cells to mineralized and nonmineralized extracellular matrices (Boissier et al., 1997; Garrioch et al., 2005), and inhibit the migration of macrophages and some tumor cells (Stevenson and Stevenson, 1986; Pietschmann et al., 1998; Hasmim et al., 2007). The decline in adhesion and migration of VSMCs suggested focal adhesions might be disrupted. Because tyrosine phosphorylation plays a critical role in the regulation of cell adhesion and migration (Panetti, 2002), we sought to investigate the phosphorylation state of regulatory proteins found within sites of attachment. A key mediator of tyrosine phosphorylation at focal adhesions is FAK, which itself becomes phosphorylated during binding of cells to the extracellular matrix (Gerthoffer and Gunst, 2001). Our data revealed that tyrosine phosphorylation of FAK was diminished in comparison with control samples. These findings indicate that zoledronate modulates the phosphorylation of FAK in VSMCs, and suggest a mechanism through which zoledronate governs adhesion and migration.

Microstructure changes of VSMCs exposed to zoledronate were observed under inverted phase contrast microscope and transmission electron microscope. More and more VSMCs changed from a bipolar appearance to a globular shape as zoledronate concentration increased from 0.1 to 100 μM. This morphological change indicated that zoledronate could interfere with VSMCs cytoskeleton. Images under transmission electron microscope confirmed this morphological change, and many electron density bodies (lysosomes) were observed in zoledronate-treated VSMCs. Lysosomes play many critical roles in biological functions, including digestion of exogenous or endogenous macromolecules, receptor recycling, repair of the plasma membrane, processing of bioactive peptide substances and antigen presentation, with acidic environment (Mullins and Bonifacino, 2001). The extracellular release of lysosomal contents are through exocytosis in both secretory and nonsecretory cells (Webste et al., 1997; Jaiswal et al., 2002). As is stated above, nitrogen-containing bisphosphonates prevents a wide variety of small intracellular G-proteins prenylation, including Rab which plays pivotal roles in vesicular transport (Zerial and McBride, 2001). Therefore, remarkable increase of lysosomes in cytoplasm might be due to inhibition of lysosomal exocytosis. Further investigation will be needed to elucidate the exact mechanism involved.

In summary, our data demonstrated that zoledronate inhibited the proliferation, adhesion and migration of VSMCs. These results contributed to a better understanding of the mechanisms by which bisophsophonate could inhibit atherosclerosis and neointimal hyperplasia.

## Acknowledgements

We would like to thank Yi-Feng Lin, Jin-Gui Mu, Xing Liu, Yong-Kang Jiang and Xiao-Hui Liao for their excellent technical support. We thank Novartis Pharma for the generous offer of zoledronate. We are grateful to Dr. Xian-Mang Pan for the critical revision of the manuscript.

## References

Andres, V., 1998. Control of vascular smooth muscle cell growth and its implication in atherosclerosis and restenosis. Int J Mol Med 2, 81–89.
Berenson, J., Ravera, C., Ma, P., Deckert, F., Sasaki, Y., Saeki, T., Takashima, S., LoRusso, P., Goodin, S., Seaman, J., Schran, H., Zhou, H., 2000. Population pharmacokinetics (PK) of Zometa. Proc Am Soc Clin Oncol 19, 209a (Abstract 814).
Boissier, S., Magnetto, S., Frappart, L., Cuzin, B., Ebetino, F.H., Delmas, P.D., Clezardin, P., 1997. Bisphosphonates inhibit prostate and breast carcinoma cell adhesion to unmineralized and mineralized bone extracellular matrices. Cancer Res 57, 3890–3894.
Caraglia, M., D'Alessandro, A.M., Marra, M., Giuberti, G., Vitale, G., Viscomi, C., Colao, A., Del Prete, S., Tagliaferri, P., Tassone, P., Budillon, A., Venuta, S., Abbruzzese, A., 2004. The farnesyl transferase inhibitor R115777 (Zarnestra) synergistically enhances growth inhibition and apoptosis induced on epidermoid cancer cells by Zoledronic acid (Zometa) and Pamidronate. Oncogene 23, 6900–6913.
Cohen-Sela, E., Rosenzweig, O., Gao, J., Epstein, H., Gati, I., Reich, R., Danenberg, H.D., Golomb, G., 2006. Alendronate-loaded nanoparticles deplete monocytes and attenuate restenosis. J Control Release 113, 23–30.
Danenberg, H.D., Fishbein, I., Gao, J., Monkkonen, J., Reich, R., Gati, I., Moerman, E., Golomb, G., 2002. Macrophage depletion by clodronate-containing liposomes reduces neointimal formation after balloon injury in rats and rabbits. Circulation 106, 599–605.
Danenberg, H.D., Golomb, G., Groothuis, A., Gao, J., Epstein, H., Swaminathan, R.V., Seifert, P., Edelman, E.R., 2003. Liposomal alendronate inhibits systemic innate immunity and reduces in-stent neointimal hyperplasia in rabbits. Circulation 108, 2798–2804.
Daoud, A.S., Frank, A.S., Jarmolych, J., Fritz, K.E., 1987. The effect of ethane-1-hydroxy-11 diphosphonate (EHDP) on necrosis of atherosclerotic lesions. Atherosclerosis 67, 41–48.
Davies, M.G., Hagen, P.O., 1994. Pathobiology of intimal hyperplasia. Br J Surg 81, 1254–1269.
Delafontaine, P., 1998. Growth factors and vascular smooth muscle cell growth responses. Eur Heart J 19, G18–22.
Epstein, H., Berger, V., Levi, I., Eisenberg, G., Koroukhov, N., Gao, J., Golomb, G., 2007. Nanosuspensions of alendronate with gallium or gadolinium attenuate neointimal hyperplasia in rats. J Control Release 117, 322–332.
Evdokiou, A., Labrinidis, A., Bouralexis, S., Hay, S., Findlay, D.M., Evdokiou, A., Labrinidis, A., Bouralexis, S., Hay, S., Findlay, D.M., 2003. Induction of cell death of human osteogenic sarcoma cells by zoledronic acid resembles anoikis. Bone 33, 216–228.
Garrioch, S., Ebetino, F.H., Rogers, M.J., 2005. Bisphosphonates prevent adhesion of breast cancer cells to bone in vitro by inhibiting protein prenylation. J Bone Miner Res 20, 1294.
Gerthoffer, W.T., Gunst, S.J., 2001. Invited review: focal adhesion and small heat shock proteins in the regulation of actin remodeling and contractility in smooth muscle. J Appl Physiol 91, 963–972.
Green, J.R., 2002. Preclinical pharmacology of zoledronic acid. Semin Oncol 29, 3–11.
Hanke, H., Strohschneider, T., Oberhoff, M., Betz, E., Karsch, K.R., 1990. Time course of smooth muscle cell proliferation in the intima and media of arteries following experimental angioplasty. Circ Res 67, 651–659.
Hasmim, M., Bieler, G., Ruegg, C., 2007. Zoledronate inhibits endothelial cell adhesion, migration and survival through the suppression of multiple, prenylation-dependent signaling pathways. J Thromb Haemost 5, 166–173.
Hoch, J.R., Stark, V.K., Van Rooijen, N., Kim, J.L., Nutt, M.P., Warner, T.F., 1999. Macrophage depletion alters vein graft intimal hyperplasia. Surgery 126, 428–437.
Hou, Y.Z., Yang, J., Zhao, G.R., Yuan, Y.J., 2004. Ferulic acid inhibits vascular smooth muscle cell proliferation induced by angiotensin II. Eur J Pharmacol 499, 85–90.
Ibrahim, A., Scher, N., Williams, G., Sridhara, R., Li, N., Chen, G., Leighton, J., Booth, B., Gobburu, J.V., Rahman, A., Hsieh, Y., Wood, R., Vause, D., Pazdur, R., 2003. Approval summary for zoledronic acid for treatment of multiple myeloma and cancer bone metastases. Clin Cancer Res 9, 2394–2399.
Jaiswal, J.K., Andrews, N.W., Simon, S.M., 2002. Membrane proximal lysosomes are the major vesicles responsible for calcium-dependent exocytosis in nonsecretory cells. J Cell Biol 159, 625–635.
Kamiya, K., Ryer, E., Sakakibara, K., Zohlman, A., Kent, K.C., Liu, B., 2007. Protein kinase C delta activated adhesion regulates vascular smooth muscle cell migration. J Surg Res 141, 91–96.
Koshiyama, H., Nakamura, Y., Tanaka, S., Minamikawa, J., 2000. Decrease in carotid intima-media thickness after 1-year therapy with etidronate for osteopenia associated with type 2 diabetes. J Clin Endocrinol Metab 85, 2793–2796.
Koutsouki, E., Beeching, C.A., Slater, S.C., Blaschuk, O.W., Sala-Newby, G.B., George, S.J., 2005. N-cadherin-dependent cell-cell contacts promote human saphenous vein smooth muscle cell survival. Arterioscler Thromb Vasc Biol 25, 982–988.
Li, Y.Y., Chang, J.W., Chou, W.C., Liaw, C.C., Wang, H.M., Huang, J.S., Wang, C.H., Yeh, K.Y., 2008. Zoledronic acid is unable to induce apoptosis, but slows tumor growth and prolongs survival for non-small-cell lung cancers. Lung Cancer 59, 180–191.
Lortholary, A., 2001. Tumor-induced hypercalcemia. A review of the treatment by bisphosphonates. Rev Med Interne 22, 648–652.
Luckman, S.P., Hughes, D.E., Coxon, F.P., Graham, R., Russell, G., Rogers, M.J., 1998. Nitrogen-containing bisphosphonates inhibit the mevalonate pathway and prevent post-translational prenylation of GTP-binding proteins, including Ras. J Bone Miner Res 13, 581–589.
Merlotti, D., Gennari, L., Martini, G., Valleggi, F., De Paola, V., Avanzati, A., Nuti, R., 2007. Comparison of different intravenous bisphosphonate regimens for Paget's disease of bone. J Bone Miner Res 22, 1510–1517.

Morla, A.O., Mogford, J.E., 2000. Control of smooth muscle cell proliferation and phenotype by integrin signaling through focal adhesion kinase. Biochem Biophys Res Commun 272, 298–302.
Mullins, C., Bonifacino, J.S., 2001. The molecular machinery for lysosome biogenesis. Bioessays 23, 333–343.
Ohtsuka, Y., Manabe, A., Kawasaki, H., Hasegawa, D., Zaike, Y., Watanabe, S., Tanizawa, T., Nakahata, T., Tsuji, K., 2005. RAS-blocking bisphosphonate zoledronic acid inhibits the abnormal proliferation and differentiation of juvenile myelomonocytic leukemia cells in vitro. Blood 106, 3134–3141.
Owens, G., Jackson, R., Lewiecki, E.M., 2007. An integrated approach: Bisphosphonate management for the treatment of osteoporosis. Am J Manag Care. 13, S290–S308.
Panetti, T.S., 2002. Tyrosine phosphorylation of paxillin, FAK, and p130CAS: effects on cell spreading and migration. Front Biosci 7, d143–d150.
Peest, D., Ganser, A., 2007. Therapy of multiple myeloma: indications and options. Internist 48, 1343.
Pietschmann, P., Stohlawetz, P., Brosch, S., Steiner, G., Smolen, J.S., Peterlik, M., 1998. The effect of alendronate on cytokine production, adhesion molecule expression, and transendothelial migration of human peripheral blood mononuclear cells. Calcif Tissue Int 63, 325–330.
Ross, R., 1997. Cellular and molecular studies of atherogenesis. Atherosclerosis 131, S3–S4.
Stevenson, P.H., Stevenson, J.R., 1986. Cytotoxic and migration inhibitory effects of bisphosphonates on macrophages. Calcif Tissue Int 38, 227–233.
Su, J.Z., Fukuda, N., Kishioka, H., Hu, W.Y., Kanmatsuse, K., 2002. Etidronate influences growth and phenotype of rat vascular smooth muscle cells. Pharmacol Res 46, 7–13.
Tassone, P., Tagliaferri, P., Viscomi, C., Palmieri, C., Caraglia, M., D'Alessandro, A., Galea, E., Goel, A., Abbruzzese, A., Boland, C.R., Venuta, S., 2003. Zoledronic acid induces antiproliferative and apoptotic effects in human pancreatic cancer cells in vitro. Br J Cancer 88, 1971–1978.
Tenenbaum, H.C., Torontali, M., Sukhu, B., 1992. Effects of bisphosphonates and inorganic pyrophosphate on osteogenesis in vitro. Bone 13, 249–255.
Van Beek, E., Pieterman, E., Cohen, L., Lowik, C., Papapoulos, S., 1999. Farnesyl pyrophosphate synthase is the molecular target of nitrogen-containing bisphosphonates. Biochem Biophys Res 264, 108–111.
Webb, D.J., Parsons, J.T., Horwitz, A.F., 2002. Adhesion assembly, disassembly and turnover in migrating cells — over and over and over again. Nat Cell Biol 4, E97–E100.
Webste, P., Ortego, J., Andrews, N.W., 1997. Lysosomes behave as Ca2+-regulated exocytic vesicles in fibroblasts and epithelial cells. J Cell Biol 137, 93–104.
Ylitalo, R., Oksala, O., Ylaherttuala, S., Ylitalo, P., 1994. Effects of clodronate (dichloromethylene bisphosphonate) on the development of experimental atherosclerosis in rabbits. J Lab Clin Med 123, 769–776.
Ylitalo, R., Monkkonen, J., Urtti, A., Ylitalo, P., 1996. Accumulation of bisphosphonates in the aorta and some other tissues of healthy and atherosclerotic rabbits. J Lab Clin Med 127, 200–206.
Ylitalo, R., Kalliovalkama, J., Wu, X.M., Kankaanranta, H., Salenius, J.P., Sisto, T., Lahteenmaki, T., Ylitalo, P., Porsti, I., 1998. Accumulation of bisphosphonates in human artery and their effects on human and rat arterial function in vitro. Pharmacol Toxicol 83, 125–131.
Zerial, M., McBride, H., 2001. Rab proteins as membrane organizers. Nat Rev Mol Cell Biol 2, 107–117.
Zhang, F.L., Casey, P.J., 1996. Protein prenylation: molecular mechanisms and functional consequences. Annu Rev Biochem 65, 241–269.